Nanotechnology, Science and Applications

Dovepress
Taylor & Francis Group

Open Access Full Text Article

ORIGINAL RESEARCH

Alternative Metallocenes in Floating Catalyst-CVD: Synthesis of Novel Carbon Nanostructures

Sandra Lepak-Kuc[1,2], Agnieszka Lekawa-Raus[2], Malgorzata Jakubowska[1,2], Krzysztof Koziol[3]

[1]Faculty of Mechanical and Industrial Engineering, Warsaw University of Technology, Warsaw, Poland; [2]Centre for Advanced Materials and Technologies (CEZAMAT), Warsaw University of Technology, Warsaw, Poland; [3]Enhanced Composites & Structures Centre, Cranfield University, Cranfield, UK

Correspondence: Agnieszka Lekawa-Raus, Centre for Advanced Materials and Technologies (CEZAMAT), Warsaw University of Technology, Warsaw, 02-822, Poland, Email agnieszka.raus@pw.edu.pl

Introduction: The floating catalyst chemical vapour deposition (FC-CVD) method is widely used for synthesising carbon nanotubes (CNTs), typically with ferrocene as the catalyst. This study explores the use of alternative, nonferrous metallocenes to investigate their impact on carbon nanostructure formation.

Methods: Six metallocenes - ferrocene, cobaltocene, ruthenocene, vanadocene, manganocene, and magnesocene - were tested under comparable FC-CVD conditions. The resulting materials were characterised using scanning electron microscopy (SEM), Raman spectroscopy, and energy-dispersive X-ray spectroscopy (EDS).

Results and Discussion: Ferrocene produced vertically aligned CNT carpets with high crystallinity. Cobaltocene and magnesocene also yielded CNTs, though less aligned and more defective. Ruthenocene and vanadocene resulted in disordered graphitic carbon without nanotube morphology, confirmed by the presence of broad D and G bands in Raman spectra. Notably, manganocene catalysed the formation of dendritic structures with oxidised and functionalised surfaces, exhibiting unique morphologies distinct from conventional CNTs.

Conclusion: These results highlight the ability of nonferrous metallocenes to direct the growth of unconventional carbon nanostructures. The findings suggest new possibilities for tailoring nanocarbon morphology through catalyst selection, particularly for applications requiring high surface area or chemical functionality.

Keywords: CVD, metallocene, catalyst, carbon nanotube, carbon nanostructure

Introduction

Chemical vapour deposition (CVD) is one of the most extensively studied methods for synthesising nanoparticles.[1,2] CVD is an exceptionally versatile method that enables the formation of a wide range of nanoparticles, including carbon nanotubes, graphene, hexagonal boron nitride, MXenes, and many more 1D and 2D materials.[3–6] Its advantages, such as simplicity, scalability, and economic efficiency, show great promise for potential industrial manufacturing of synthesized materials. Since its discovery over 50 years ago, many types of CVD processes have been distinguished, including water-assisted CVD,[7,8] plasma-enhanced CVD (PE-CVD),[9,10] metal-organic CVD (MOCVD)[11] or floating catalyst CVD (FC-CVD).[12,13] The latter one, FC-CVD, has gained substantial interest due to the unique opportunities it offers in the synthesis of carbon nanotubes,[14–17] particularly enabling a continuous one-step synthesis of CNT macroarchitectures such as CNT fibres and films, as well as CNT arrays.[4,18,19] Furthermore, FC-CVD offers the possibility of controlling the nanostructure of CNTs. The process can be optimised to synthesise single-walled carbon nanotubes (SWCNT),[17,20,21] double-walled carbon nanotubes (DWCNT)[22] and multi-walled carbon nanotubes (MWCNT),[23] as well as provide control over the length, chirality or doping of the nanotubes.[20,24,25] Understanding that CVD processes are capable of synthesising

Received: 18 January 2025
Accepted: 8 July 2025
Published: 7 September 2025

Graphical Abstract

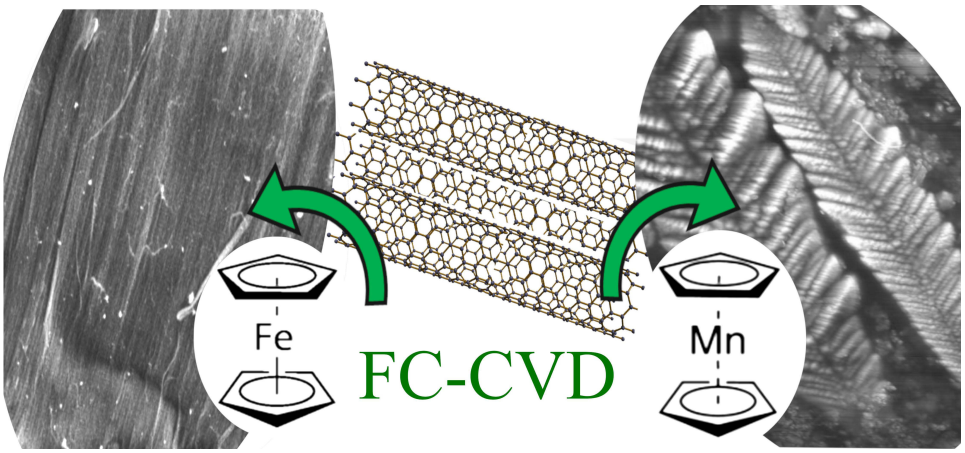

a wide range of nanoparticles, it is reasonable to anticipate that FC-CVD might offer capabilities beyond merely synthesising traditional carbon nanotubes, through adjustments in process parameters and feedstocks. In the quest for precise synthesis of CNTs, a plethora of process variables have been explored, including temperature settings, types and flow rates of gases, reactor configurations, carbon sources, sulphur compounds, and, lastly, catalysts.[17,24,25] Regarding the latter parameter, one of the earliest studies of FC-CVD process by Sen et al focused on the use of metallocenes.[26] The metallocenes tested in this research paper included ferrocene, cobaltocene and nickelocene. All these metallocenes were further studied separately as well as in mixtures.[27,28] The key studies relied on using an iron catalyst derived from ferrocene[20,23,29–31] due to much better yield and quality of CNTs, improved growth rate and scalability of the process.[32] Nonetheless, it has been shown that the use of cobaltocene may lead to the formation of interesting structures such as cup-stacked carbon nanotubes[27] as well as improved catalytic activity in the case of cobaltocene and nickelocene mixtures with ferrocene.[28,33] This indicates that the use of other nonferrous metallocenes may alter carbon nanostructure synthesis routes, potentially yielding novel nanomorphologies. To explore this opportunity, in this work, we conducted a series of experiments using six compounds from the metallocene family: Ferrocene, Cobaltocene, Ruthenocene, Vanadocene, Manganocene, and Magnesocene as catalyst sources in FC-CVD syntheses of carbon nanomaterials. These experiments revealed the emergence of novel structures, diverging from conventional carbon nanotubes, some featuring distinctive shapes. In particular, the unique dendritic morphologies obtained with manganocene suggest potential applications in areas such as energy storage, sensing, or printed electronics, where high surface area and oxygen functionality are advantageous.

Results and Discussion

The first experiment aimed to obtain the reference data for further studies presented in this work. The experiment followed the procedure identified in the literature to be the most efficient, yielding carbon nanotube arrays of the highest purity.[34–36] The CNT arrays were synthesised using a solution of 5 wt.% of ferrocene in toluene. The preheater temperature was set to 170°C. The evaporating feedstock has been injected into the hot zone of the reactor and transported with the argon flow set at 1 L/min. The synthesis has been performed at 760°C. SEM images and Raman spectrum of synthesised CNT structure are presented in Figure 1.

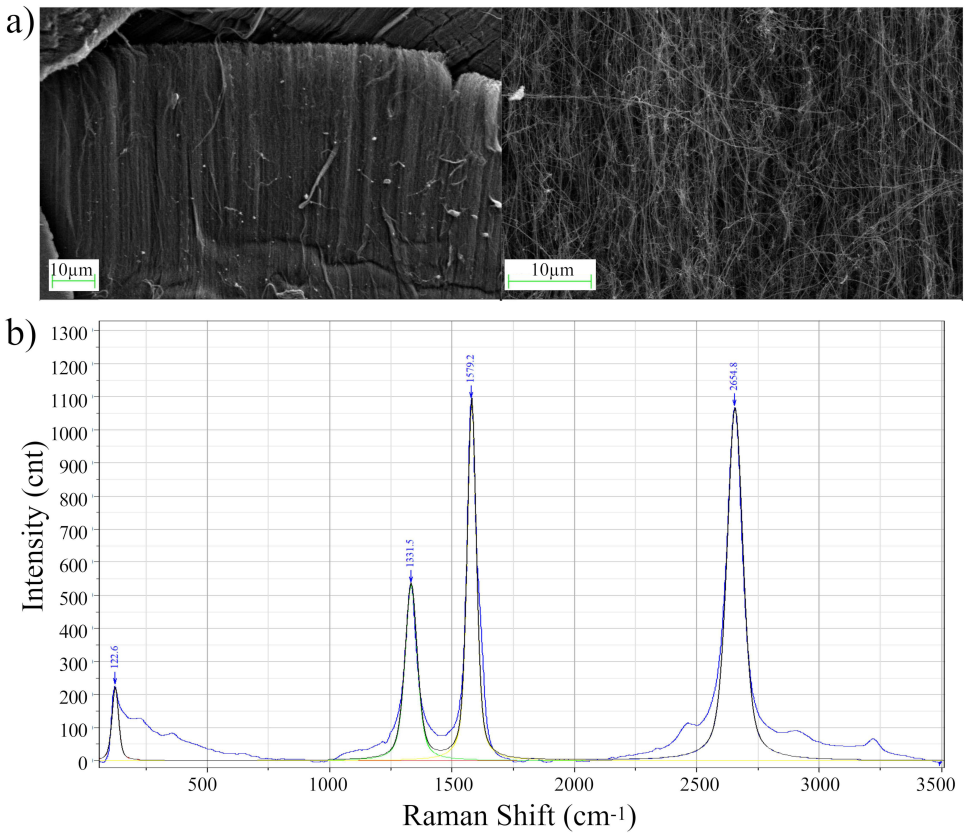

Figure 1 Scanning electron microscopy (**a**) and Raman spectrum (**b**) of carbon nanotube array structure obtained in the dedicated process with the ferrocene as the catalyst.

As is shown in Figure 1 the FC-CVD method allowed obtaining a regular array structure of carbon nanotubes. Individual carbon nanotubes had typical diameters in the range of several tens of nanometers. The height of the arrays was about one millimetre. Such a result ranks very well among the CNT array structures described in the literature[34–38] and proves that the applied parameters of the process were well-adjusted.

The presented Raman spectrum shows all features characteristic of Raman spectroscopy of CNT structures. Radial breathing mode (RBM) is visible at low frequencies, suggesting that the synthesised material includes single-wall nanotubes (SWNT). Around 1330 cm^{-1}, a D-band peak appears, which is typically observed in all graphitic structures that contain some impurities or defects that break the sp^2 carbon structure symmetry.[39–41] Next, at the frequency of ~1580 cm^{-1} G-band, originating from carbon atom vibrations is visible. The overtone of the D-band, known as the 2D-band, is also visible on the analysed spectrum at ~2650 cm^{-1}. All the peaks are sharp and well-located, which proves the good quality and purity of the material.

In the following syntheses, the ferrocene catalyst precursor has been replaced by other metallocenes - Cobaltocene, Ruthenocene, Vanadocene, Manganocene and Magnesocene. The process conditions which were found to yield the best CNT arrays for ferrocene-based synthesis were assumed to be the starting point for other metallocene syntheses. However, some procedure parameters had to be adjusted to accommodate the melting points and solubility of the new catalysts being tested. These compounds share a closely similar structure. All of them are bis(cyclopentadienyl)metal structures, however, they exhibit some differences, for example, having varying melting points with values: 172.5°C, 173°C, 194°C, 165°C, 173°C, 176°C for Ferrocene, Cobaltocene, Ruthenocene, Vanadocene, Manganocene and Magnesocene, respectively.

For all catalysts, a feedstock of 5 wt.% metallocene in toluene was prepared. During the preparation of the feedstock, different solubilities of individual metallocenes were observed. This resulted in an extended sonication-assisted dissolution time, up to an hour, in the case of the Vanadocene and Manganocene.

https://doi.org/10.2147/NSA.S518220

For all the tested metallocenes, experiments were first carried out with the process parameters used for ferrocene (preheater temperature of 170°C, oven temperature - 760°C). Next, the temperatures were modified in the range of 650–850°C for the furnace, and 150–200°C at the preheater and product deposition on quartz glass was investigated. For most of the catalysts tested, modifications of process temperatures did not improve the deposition of the products. However, the significant difference in the melting point of ruthenocene compared to ferrocene necessitated an increase of the temperature of the preheater to 200°C and the temperature of the actual pyrolysis to 850°C.

All deposits obtained in the syntheses were subject to scanning electron microscopy (SEM) and Raman spectroscopy analysis. SEM images of the obtained nano and micromaterials are presented in Figure 2.

As shown in Figure 2a and b, the use of cobaltocene as a reaction catalyst formed nanotube structures. However, the nanotubes are not arranged in a regular array structure, as is the case with iron catalysts.

In the case of the Magnesocene, individual nanotube structures can be seen at higher magnification (Figure 2d). However, their number is negligible and their length is much shorter than for the Cobaltocene. In the case of the catalyst in the form of both a Vanadium compound (Figure 2e and f) and a Ruthenium compound (Figure 2g and h), no nanotube structures are visible. The structures visible in the obtained images are rather similar to graphite forms decorated with metal catalysts. The analysis of SEM images seems to indicate that the most interesting material is the product of the manganocene-catalysed reaction (Figure 2i and j). Dendritic structures resembling fern leaves were obtained.

The observed variations in carbon nanostructure morphology can be attributed to the intrinsic properties of the metallocene catalysts used. Thermal decomposition temperatures play a crucial role; metallocenes with lower decomposition points activate earlier, leading to different catalyst particle sizes and distributions. Moreover, the strength of metal-carbon interactions influences the formation of metal carbides, which serve as active sites for carbon growth. For instance, nickel's strong affinity for carbon facilitates the formation of stable carbides, promoting the growth of well-structured carbon nanotubes. In contrast, metals with weaker carbon interactions may lead to amorphous carbon structures. Additionally, the electronic configuration and oxidation state of the metal center affect catalytic activity and selectivity, further influencing the morphology of the synthesized carbon materials.

All obtained materials were also analysed by Raman spectroscopy for chemical and structural identification (Figure 3a–e). Due to the unusual and intriguing structure of the manganocene-catalysed material, it was additionally subjected to an Energy Dispersive Spectroscopy (EDS) analysis to characterise the elemental composition (Figure 3f).

The Raman spectra presented in (Figure 3a–e) seem to lead to conclusions consistent with the analysis of SEM images. For the structures obtained for the cobaltocene (Figure 3a), magnesocene (Figure 3b), ruthenocene (Figure 3c) and vanadocene (Figure 3d) catalysis, the Raman spectra show the D and G bands characteristic of nanocarbon structures, with wavenumbers of around 1300 and around 1580 cm^{-1}, respectively. The bands in these positions are characteristic of sp^2 hybridized materials. Thus, both nanotube structures and graphene/graphite can be present in the samples. Therefore, to analyse the composition, it is necessary to correlate the results of Raman spectroscopy with SEM images. In the case of cobalt (Figure 3a) and magnesium (Figure 3b) based catalysts, the images clearly show the presence of carbon nanotubes. The G-band to the D-band intensity ratio is often mentioned as a useful tool for determining the quality of produced carbon nanotubes. The D-band is associated with defects within the graphic lattice or even with amorphous carbons. The better the purity and quality of the nanotubes, the higher the value of the G:D ratio is observed.[42] Therefore, both the cobaltocene and magnesocene carbon nanotubes contain numerous defects, which is also consistent with the results of the SEM analysis.

Furthermore, taking into account both the SEM imaging results and the presence of the typical G and D bands in Raman spectroscopy for materials catalysed by ruthenocene (Figure 3c) and vanadocene (Figure 3d), it can be concluded that graphite structures were obtained, probably functionalised to some extent by the presence of ruthenium and vanadium elements, respectively.

Even though the presence, shape and location of the characteristic bands provide a large amount of information about the carbon material, there is a large discrepancy in the literature regarding the Raman spectra of various graphite systems, eg relatively newly produced graphitised structures reduced from oxides, wrinkled or functionalised sp^2-bonded carbon materials.[43–46] For graphene, a strong share of the 2D band is usually observed, which is not observed for the materials tested here. Yet, it is not difficult to find reports in which the 2D band is very broadened and not very intense, as well as

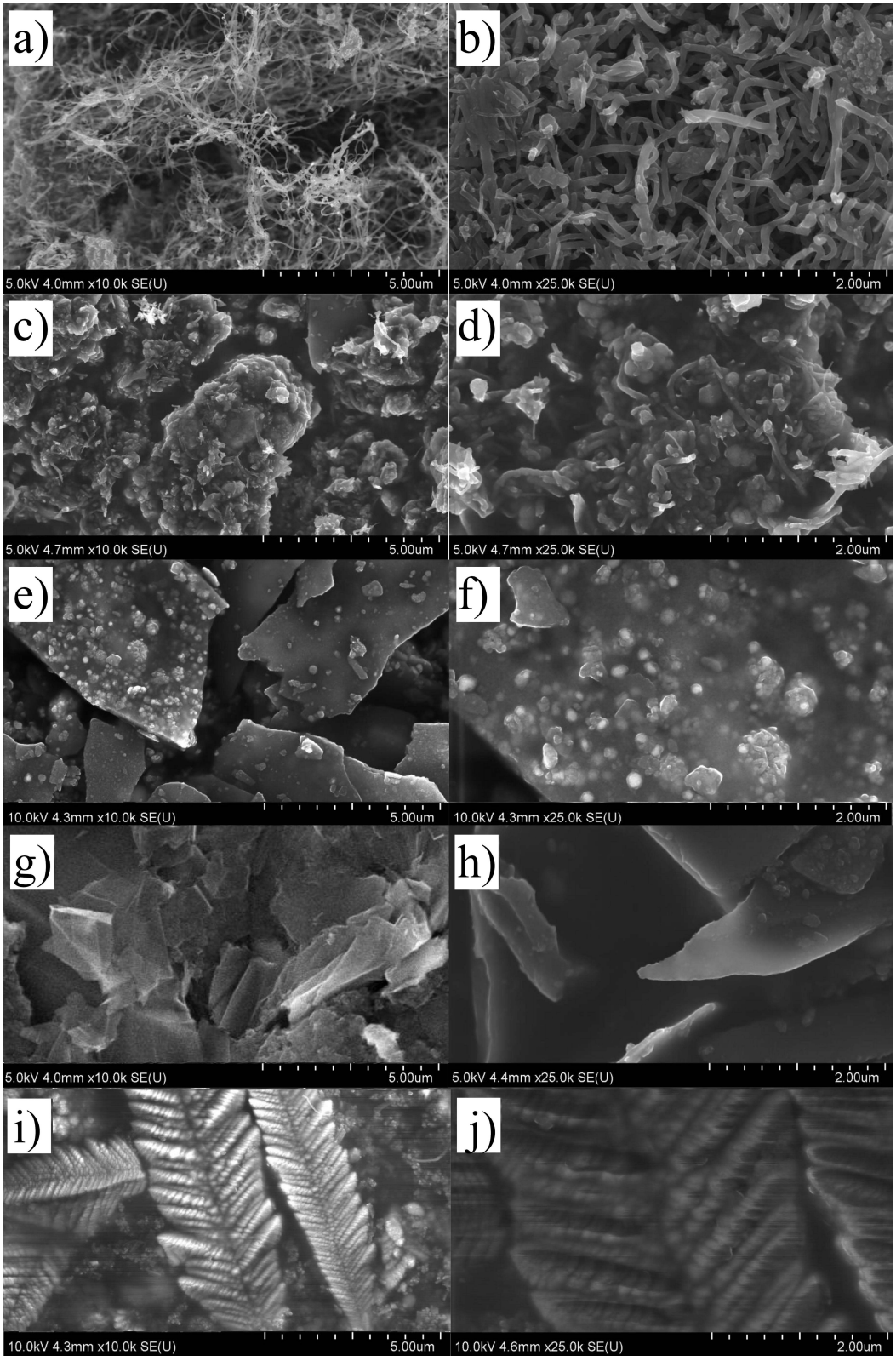

Figure 2 Scanning electron microscopy images of carbon structures synthesised with the usage of (**a** and **b**) cobaltocene, (**c** and **d**) magnesocene, (**e** and **f**) vanadocene, (**g** and **h**) ruthenocene, (**i** and **j**) manganocene as a catalyst. For each catalyst, images are presented at 10,000× (left) and 25,000× (right) magnification to allow consistent comparison of morphological features.

https://doi.org/10.2147/NSA.S518220

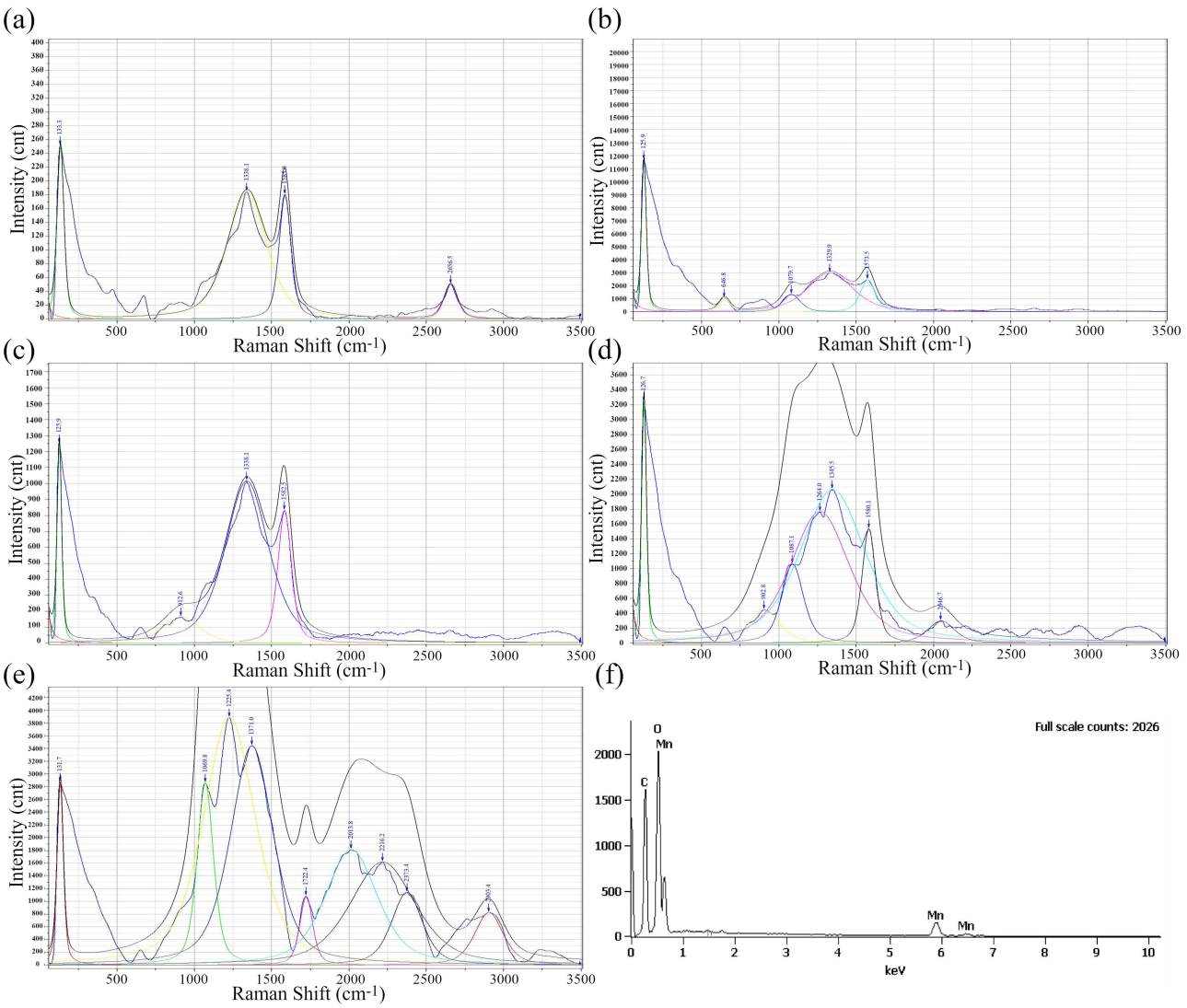

Figure 3 Raman spectra of carbon structures synthesised with the usage of (**a**) cobaltocene, (**b**) magnesocene, (**c**) vanadocene, (**d**) ruthenocene, (**e**) manganocene as a catalyst. Energy Dispersive Spectroscopy analysis of the structure synthesised with manganocene as a catalyst (**f**).

in which the 2D band is omitted at all.[46–49] In general, Raman spectra of graphitised structures depend not only on the number of layers or the number of graphitisation disturbances but also largely on their functionalisation, production method or substrate.

Among all tested materials the most intriguing and thought-provoking is the one catalysed by the manganocene (Figure 3e). With the aim to better analyse the surprising SEM images and the diversity of bands in Raman spectroscopy, this material was also subjected to elemental composition analysis using EDS (Figure 3f). As shown by the result of this test, the compound synthesized as a result of the Manganocene catalysed reaction consists of carbon, manganese and oxygen. This most likely indicates that nanocarbon structures, built on the manganese catalyst were obtained, which are further functionalized with oxygen from the air. This information allows a better understanding of the plurality of bands in the Raman spectrum.

A number of bands can be observed in the Raman spectrum of this material, some of which can be sorted into groups. The first visible signal is around 131 cm^{-1}, the intense band in this position for carbon structures is often associated with the presence of single-walled nanotubes. Between 1069 cm^{-1} and 1371 cm^{-1}, a group of three bands is visible, and these are the most intense peaks of the analysed spectrum. The location of these bands, namely in the vicinity of the D band, may indicate that we are dealing with a highly disturbed structure of nanotubes. For wavenumber 1722 cm^{-1}, a single

band is visible, followed by another triplet of bands at positions between 2013 cm^{-1} and 2373 cm^{-1}. The last visible band appears at the wavenumber of 2903 cm^{-1}. The analysis of such arranged strands is not easy. Both the SEM images, which show the extremely complex architecture of the material, and the EDS results, which show a small number of constituent elements, should be considered. Bands in the range 1650–1750 cm^{-1} indicate the presence of carbon-oxygen double bonds and the bands in the range 2100–2300 cm^{-1} indicate the presence of carbon-carbon triple bonds. The last band, on the other hand, indicates carbon-hydrogen vibrations.[50] The structure obtained is probably a nanocarbon structure with a strong disturbance of the graphite structure, for example, due to the complicated structure and the related series of carbon bonds. In addition, this structure is most likely functionalized with oxygen, which presumably happened due to the oxidation of the carbon structures by the manganese catalyst.

While this study focused on the synthesis and structural analysis of carbon nanomaterials derived from various metallocene catalysts, the unique features of the manganese-catalysed dendritic structures—such as high surface complexity, presence of oxygen functionalities (as suggested by EDS and Raman), and hierarchical morphology—make them promising candidates for further functional evaluation.

In particular, such materials could be explored in printed electronics, as novel functional fillers or electrodes in conductive inks and pastes,[51,52] or in electrochemical sensing platforms,[53,54] where surface functional groups can enhance molecular binding. Moreover, their complex surface topology and redox-active components suggest potential in energy storage devices,[55] including supercapacitors[56] and battery electrodes.[57] These possibilities position the synthesised materials as intriguing subjects for future application-driven studies.

Conclusions

Unique properties of nanoscopic carbon materials lead to extensive works of both the new materials among this family and other synthesis possibilities of known materials. To fulfil both of those trends we presented research on the capabilities of CNT arrays-dedicated furnace, on the synthesis of either nanotube with better alignment or new carbon nanostructures. The use of metallocenes as catalysts was associated with the proven effectiveness of ferrocene in the synthesis of good quality vertically aligned carbon nanotubes carpets. Conducted tests showed that catalysis by cobaltocene and magnesocene allows obtaining the structure of nanotubes. However, these are not regularly arranged parallel structures and graphitization is strongly disturbed. The defects are stronger for the catalysis with the magnesium compound. The materials synthesized by the vanadocene and ruthenocene catalysis did not show the structure of the nanotubes. However, the Raman spectra of these materials reveal the G - and D - bands characteristic of the graphite structures. The observations of the scanning electron microscopy images allow confirming the presence of graphite structures. The manganocene-catalysed reaction allows for obtaining very interesting structures resembling ferns. Based on the conducted material analysis we were able to characterize the material as oxidized and functionalized carbon structures. The manganocene-catalysed reaction allows for obtaining very interesting structures resembling ferns. Based on the conducted material analysis we were able to characterize the material as oxidized and functionalized carbon structures.

The research conducted allowed us to obtain interesting materials. It was shown that the growth of nanotube structures does not occur for the entire family of metallocenes and that intriguing and unusual structures can be obtained. These findings highlight the potential of nonferrous metallocenes to diversify the morphology of carbon nanomaterials beyond traditional CNTs. Considering the unique features and potential applications of these nanostructures, particularly those derived from manganocene, it would be highly valuable to pursue further studies. Future experimental research should focus on optimising synthesis conditions, assessing reproducibility, addressing the scalability of material manufacturing, as well as evaluating the functional performance of these novel nanostructures, including the testing of electrical, thermal and mechanical properties, and chemical reactivity. Full understanding of the mechanisms responsible for the synthesis of novel nanomaterials could be gained through the simultaneous atomistic modelling of the synthesis reactions.

Experimental Section

Materials: In all experiments, toluene was used as a carbon substrate. The tested catalysts included Ferrocene, Cobaltocene, Ruthenocene, Vanadocene, Manganocene, and Magnesocene. Toluene and Ferrocene were purchased from Sigma Aldrich, UK. Other metallocenes were purchased from Strem Chemicals, Inc., UK.

Synthesis

Carbon nanomaterials were synthesized using the previously described chemical vapour deposition process, tailored specifically for the synthesis of carbon nanotube arrays.[58] Briefly, the setup comprised a horizontal tube furnace capable of reaching temperatures up to 900°C, a liquid feedstock injector heated to 200°C, a source of argon gas, and an exhaust filtering system. During a standard CNT synthesis process, the liquid feedstock, comprised of a carbon source and a catalyst source, is heated and then injected into the reactor's main zone with a flow of argon. Within the reactor's hot zone, the feedstock undergoes pyrolysis. Iron catalysts deposit on the walls of the quartz tube, initiating the growth of CNTs in the form of arrays. All syntheses were performed in triplicate to confirm reproducibility. Representative results are shown.

Solutions Preparation

The metallocene solutions in toluene were prepared by weighing the desired amount of metallocene and toluene and their homogenization using a VCX 750 ultrasonic homogeniser until visible dissolution of metallocene in toluene. 10 minutes each for Ferrocene, Cobaltocene, Ruthenocene, Magnesocene. 60 minutes each for, Vanadocene, and Manganocene.

Characterization

The Raman analysis was made on the Horiba LabRam 300 spectrometer with a 17 mW, 633 nm red laser. The analysis software was Lab Spec 5. Scanning Electron Microscopy of the reference CNT array was carried out using a Carl Zeiss Auriga 60 high-resolution scanning electron microscope with an accelerating voltage of 8 kV. Structural investigations were combined with advanced energy-dispersive spectroscopy analysis.

Funding

This research was funded by Warsaw University of Technology IDUB, POB Materials Technologies – 3 ADVANCED grant no1820/359/Z01/POB5/2021.

Disclosure

The authors report no conflicts of interest in this work.

References

1. Allaedini G, Tasirin SM, Aminayi P. Synthesis of CNTs via Chemical Vapor Deposition of Carbon Dioxide as a Carbon Source in the Presence of NiMgO. *J Alloys Compd*. 2015;647:809–814. doi:10.1016/j.jallcom.2015.06.012
2. Kumar M, Ando Y. Chemical Vapor Deposition of Carbon Nanotubes: a Review on Growth Mechanism and Mass Production. *J Nanosci Nanotechnol*. 2010;10(6):3739–3758. doi:10.1166/jnn.2010.2939
3. Hussein FH, Abdulrazzak FH. Synthesis of Carbon Nanotubes by Chemical Vapor Deposition. In: *Nanomaterials: Biomedical, Environmental, and Engineering Applications*. John Wiley & Sons, Ltd. 2018:105–132. doi:10.1002/9781119370383.ch4
4. Uchida Y, Kawahara K, Fukamachi S, Ago H. Chemical Vapor Deposition Growth of Uniform Multilayer Hexagonal Boron Nitride Driven by Structural Transformation of a Metal Thin Film. *ACS Appl Electron Mater*. 2020;2(10):3270–3278. doi:10.1021/acsaelm.0c00601
5. Fan Y, Li L, Zhang Y, Zhang X, Geng D, Hu W. Recent Advances in Growth of Transition Metal Carbides and Nitrides (MXenes) Crystals. *Adv Funct Mater*. 2022;32(16):2111357. doi:10.1002/adfm.202111357
6. Bhowmik S, Govind Rajan A. Chemical Vapor Deposition of 2D Materials: a Review of Modeling, Simulation, and Machine Learning Studies. *iScience*. 2022;25(3):103832. doi:10.1016/j.isci.2022.103832
7. Hata K, Futaba DN, Mizuno K, Namai T, Yumura M, Iijima S. Water-Assisted Highly Efficient Synthesis of Impurity-Free Single-Walled Carbon Nanotubes. *Science*. 2004;306(5700):1362–1364. doi:10.1126/science.1104962
8. Patole SP, Alegaonkar PS, Lee H-C, Yoo J-B. Optimization of Water Assisted Chemical Vapor Deposition Parameters for Super Growth of Carbon Nanotubes. *Carbon*. 2008;46(14):1987–1993. doi:10.1016/j.carbon.2008.08.009
9. Wu Y, Qiao P, Chong T, Shen Z. Carbon Nanowalls Grown by Microwave Plasma Enhanced Chemical Vapor Deposition. *Adv Mater*. 2002;14(1):64–67. doi:10.1002/1521-4095(20020104)14:1<64::AID-ADMA64>3.0.CO;2-G

10. Li Y, Mann D, Rolandi M, et al. Preferential Growth of Semiconducting Single-Walled Carbon Nanotubes by a Plasma Enhanced CVD Method. *Nano Lett*. 2004;4(2):317–321. doi:10.1021/nl035097c
11. Lee DH, Sim Y, Wang J, Kwon S-Y. Metal–Organic Chemical Vapor Deposition of 2D van Der Waals Materials—The Challenges and the Extensive Future Opportunities. *APL Mater*. 2020;8(3):030901. doi:10.1063/1.5142601
12. Zhou Z, Ci L, Song L, et al. Producing Cleaner Double-Walled Carbon Nanotubes in a Floating Catalyst System. *Carbon*. 2003;41(13):2607–2611. doi:10.1016/S0008-6223(03)00336-1
13. Zhou Z, Ci L, Chen X, et al. Controllable Growth of Double Wall Carbon Nanotubes in a Floating Catalytic System. *Carbon*. 2003;41(2):337–342. doi:10.1016/S0008-6223(02)00295-6
14. Nasibulin AG, Moisala A, Jiang H, Kauppinen EI. Carbon Nanotube Synthesis from Alcohols by a Novel Aerosol Method. *J Nanopart Res*. 2006;8 (3):465–475. doi:10.1007/s11051-005-9027-8
15. Pinault M, Pichot V, Khodja H, Launois P, Reynaud C, Mayne-L'Hermite M. Evidence of Sequential Lift in Growth of Aligned Multiwalled Carbon Nanotube Multilayers. *Nano Lett*. 2005;5(12):2394–2398. doi:10.1021/nl051472k
16. Zhang Q, Wang D-G, Huang J-Q, et al. Dry Spinning Yarns from Vertically Aligned Carbon Nanotube Arrays Produced by an Improved Floating Catalyst Chemical Vapor Deposition Method. *Carbon*. 2010;48(10):2855–2861. doi:10.1016/j.carbon.2010.04.017
17. Barnard JS, Paukner C, Koziol KK. The Role of Carbon Precursor on Carbon Nanotube Chirality in Floating Catalyst Chemical Vapour Deposition. *Nanoscale*. 2016;8(39):17262–17270. doi:10.1039/C6NR03895F
18. Lekawa-Raus A, Patmore J, Kurzepa L, Bulmer J, Koziol K. Electrical Properties of Carbon Nanotube Based Fibers and Their Future Use in Electrical Wiring. *Adv Funct Mater*. 2014;24(24):3661–3682. doi:10.1002/adfm.201303716
19. Taborowska P, Giżewski T, Patmore J, Janczak D, Jakubowska M, Lekawa-Raus A. Spun Carbon Nanotube Fibres and Films as an Alternative to Printed Electronic Components. *Materials*. 2020;13(2):431. doi:10.3390/ma13020431
20. Sundaram RM, Koziol KKK, Windle AH. Continuous Direct Spinning of Fibers of Single-Walled Carbon Nanotubes with Metallic Chirality. *Adv Mater Weinheim*. 2011;23(43):5064–5068. doi:10.1002/adma.201102754
21. Paukner C, Koziol KKK. Ultra-Pure Single Wall Carbon Nanotube Fibres Continuously Spun without Promoter. *Sci Rep*. 2014;4(1):3903. doi:10.1038/srep03903
22. Dong L, Park JG, Leonhardt BE, Zhang S, Liang R. Continuous Synthesis of Double-Walled Carbon Nanotubes with Water-Assisted Floating Catalyst Chemical Vapor Deposition. *Nanomaterials*. 2020;10(2):365. doi:10.3390/nano10020365
23. Koziol K, Vilatela J, Moisala A, et al. High-Performance Carbon Nanotube Fiber. *Science*. 2007;318(5858):1892–1895. doi:10.1126/science.1147635
24. Hou P-X, Zhang F, Zhang L, Liu C, Cheng H-M. Synthesis of Carbon Nanotubes by Floating Catalyst Chemical Vapor Deposition and Their Applications. *Adv Funct Mater*. 2022;32(11):2108541. doi:10.1002/adfm.202108541
25. Boncel S, Pattinson SW, Geiser V, Shaffer MSP, Koziol KKK. En Route to Controlled Catalytic CVD Synthesis of Densely Packed and Vertically Aligned Nitrogen-Doped Carbon Nanotube Arrays. *Beilstein J Nanotechnol*. 2014;5(1):219–233. doi:10.3762/bjnano.5.24
26. Sen R, Govindaraj A, Rao CNR. Carbon Nanotubes by the Metallocene Route. *Chem Phys Lett*. 1997;267(3):276–280. doi:10.1016/S0009-2614(97)00080-8
27. Singh C, Quested T, Boothroyd CB, et al. Synthesis and Characterization of Carbon Nanofibers Produced by the Floating Catalyst Method. *J Phys Chem B*. 2002;106(42):10915–10922. doi:10.1021/jp026159a
28. Chauhan D, Pujari A, Zhang G, Dasgupta K, Shanov VN, Schulz MJ. Effect of a Metallocene Catalyst Mixture on CNT Yield Using the FC-CVD Process. *Catalysts*. 2022;12(3):287. doi:10.3390/catal12030287
29. Karaeva AR, Urvanov SA, Kazennov NV, Mitberg EB, Mordkovich VZS. Structure and Electrical Resistivity of Carbon Nanotubes Synthesized over Group VIII Metallocenes. *Nanomaterials*. 2020;10(11):2279. doi:10.3390/nano10112279
30. Li Y-L, Kinloch IA, Windle AH. Direct Spinning of Carbon Nanotube Fibers from Chemical Vapor Deposition Synthesis. *Science*. 2004;304 (5668):276–278. doi:10.1126/science.1094982
31. Motta M, Moisala A, Kinloch IA, Windle AH. High Performance Fibres from 'Dog Bone' Carbon Nanotubes. *Adv Mater*. 2007;19(21):3721–3726. doi:10.1002/adma.200700516
32. Kim NS, Lee YT, Park J, et al. Dependence of the Vertically Aligned Growth of Carbon Nanotubes on the Catalysts. *J Phys Chem B*. 2002;106 (36):9286–9290. doi:10.1021/jp021018u
33. Lim YD, Avramchuck AV, Grapov D, et al. Enhanced Carbon Nanotubes Growth Using Nickel/Ferrocene-Hybridized Catalyst. *ACS Omega*. 2017;2(9):6063–6071. doi:10.1021/acsomega.7b00858
34. Bronikowski MJ. CVD Growth of Carbon Nanotube Bundle Arrays. *Carbon*. 2006;44(13):2822–2832. doi:10.1016/j.carbon.2006.03.022
35. Kinloch IA, Shaffer MSP, Lam YM, Windle AH. High-Throughput Screening for Carbon Nanotube Production. *Carbon*. 2004;42(1):101–110. doi:10.1016/j.carbon.2003.10.004
36. Gommes C, Blacher S, Bossuot C, Marchot P, Nagy J, Pirard J-P. Influence of the Operating Conditions on the Production Rate of Multi-Walled Carbon Nanotubes in a CVD Reactor. *Carbon*. 2004;42(8):1473–1482. doi:10.1016/j.carbon.2004.01.063
37. Kim D-H, Jang H-S, Kim C-D, et al. Dynamic Growth Rate Behavior of a Carbon Nanotube Forest Characterized by in Situ Optical Growth Monitoring. *Nano Lett*. 2003;3(6):863–865. doi:10.1021/nl034212g
38. Yun Y, Shanov V, Tu Y, Subramaniam S, Schulz MJ. Growth Mechanism of Long Aligned Multiwall Carbon Nanotube Arrays by Water-Assisted Chemical Vapor Deposition. *J Phys Chem B*. 2006;110(47):23920–23925. doi:10.1021/jp057171g
39. Dresselhaus MS, Dresselhaus G, Saito R, Jorio A. Raman Spectroscopy of Carbon Nanotubes. *Phys Rep*. 2005;409(2):47–99. doi:10.1016/j.physrep.2004.10.006
40. Saito R, Hofmann M, Dresselhaus G, Jorio A, Dresselhaus MS. Raman Spectroscopy of Graphene and Carbon Nanotubes. *Adv Phys*. 2011;60 (3):413–550. doi:10.1080/00018732.2011.582251
41. Dresselhaus MS, Dresselhaus G, Jorio A, Souza Filho AG, Saito R. Raman Spectroscopy on Isolated Single Wall Carbon Nanotubes. *Carbon*. 2002;40(12):2043–2061. doi:10.1016/S0008-6223(02)00066-0
42. Thostenson ET, Ren Z, Chou T-W. Advances in the Science and Technology of Carbon Nanotubes and Their Composites: a Review. *Compos Sci Technol*. 2001;61(13):1899–1912. doi:10.1016/S0266-3538(01)00094-X

43. Kaniyoor A, Ramaprabhu S. A Raman Spectroscopic Investigation of Graphite Oxide Derived Graphene. *AIP Adv*. 2012;2(3):032183. doi:10.1063/1.4756995
44. Subrahmanyam KS, Vivekchand SRC, Govindaraj A, Rao CNR. A Study of Graphenes Prepared by Different Methods: characterization, Properties and Solubilization. *J Mater Chem*. 2008;18(13):1517–1523. doi:10.1039/B716536F
45. Magedov IV, Frolova LV, Ovezmyradov M, Bethke D, Shaner EA, Kalugin NG. Benzyne-Functionalized Graphene and Graphite Characterized by Raman Spectroscopy and Energy Dispersive X-Ray Analysis. *Carbon*. 2013;54:192–200. doi:10.1016/j.carbon.2012.11.025
46. Kudin KN, Ozbas B, Schniepp HC, Prud'homme RK, Aksay IA, Car R. Raman Spectra of Graphite Oxide and Functionalized Graphene Sheets. *Nano Lett*. 2008;8(1):36–41. doi:10.1021/nl071822y
47. Al-Mashat L, Shin K, Kalantar-zadeh K, et al. Graphene/Polyaniline Nanocomposite for Hydrogen Sensing. *J Phys Chem C*. 2010;114(39):16168–16173. doi:10.1021/jp103134u
48. Abdelsayed V, Moussa S, Hassan HM, Aluri HS, Collinson MM, El-Shall MS. Photothermal Deoxygenation of Graphite Oxide with Laser Excitation in Solution and Graphene-Aided Increase in Water Temperature. *J Phys Chem Lett*. 2010;1(19):2804–2809. doi:10.1021/jz1011143
49. Sun S, Wu P. Competitive Surface-Enhanced Raman Scattering Effects in Noble Metal Nanoparticle-Decorated Graphene Sheets. *Phys Chem Chem Phys*. 2011;13(47):21116–21120. doi:10.1039/C1CP22727K
50. Ramansystems. Welcome to Ramansystems - Raman Frequencies. Available from: http://ramansystems.com/english/raman%20frequencies.htm. Accessed Dec 1, 2021.).
51. Janczak D, Wójkowska K, Raczyński T, et al. Development of Highly Stretchable Ag-MWCNT Composite for Screen-Printed Textile Electronics with Improved Mechanical and Electrical Properties. *NSA*. 2024;17:289–302. doi:10.2147/NSA.S493579
52. Janczak D, Słoma M, Wróblewski G, Młożniak A, Jakubowska M. Screen-Printed Resistive Pressure Sensors Containing Graphene Nanoplatelets and Carbon Nanotubes. *Sensors*. 2014;14(9):17304–17312. doi:10.3390/s140917304
53. Yáñez-Sedeño P, Pingarrón JM, Riu J, Rius FX. Electrochemical Sensing Based on Carbon Nanotubes. *TrAC Trends in Analytical Chemistry*. 2010;29(9):939–953. doi:10.1016/j.trac.2010.06.006
54. Saleh Ahammad AJ, Lee -J-J, Rahman Md A. Electrochemical Sensors Based on Carbon Nanotubes. *Sensors*. 2009;9(4):2289–2319. doi:10.3390/s90402289
55. Olabi AG, Abdelkareem MA, Wilberforce T, Sayed ET. Application of Graphene in Energy Storage Device – a Review. *Renewable Sustainable Energy Rev*. 2021;135:110026. doi:10.1016/j.rser.2020.110026
56. Chen T, Dai L. Carbon Nanomaterials for High-Performance Supercapacitors. *Mater Today*. 2013;16(7):272–280. doi:10.1016/j.mattod.2013.07.002
57. Zhu S, Sheng J, Chen Y, Ni J, Li Y. Carbon Nanotubes for Flexible Batteries: recent Progress and Future Perspective. *Natl Sci Rev*. 2020;8(5):nwaa261. doi:10.1093/nsr/nwaa261
58. Pattinson SW, Prehn K, Kinloch IA, et al. The Life and Death of Carbon Nanotubes. *RSC Adv*. 2012;2(7):2909–2913. doi:10.1039/C2RA00660J